Soft Matter

Merging Versatile Polymer Chemistry with Multifunctional Nanoparticles: An Overview of Crosslinkable Aromatic Polyester Matrix Nanocomposites

Journal:	*Soft Matter*
Manuscript ID	SM-REV-10-2019-002129.R1
Article Type:	Review Article
Date Submitted by the Author:	24-Dec-2019
Complete List of Authors:	Bakir, Mete; University of Illinois at Urbana-Champaign, Mechanical Science and Engineering Meyer, Jacob ; University of Illinois at Urbana-Champaign, Mechanical Science and Engineering Pang, Siyuan; University of Illinois at Urbana-Champaign, Mechanical Science and Engineering Economy, James; University of Illinois at Urbana-Champaign, Materials Science and Engineering Jasiuk, Iwona ; University of Illinois at Urbana-Champaign, Mechanical Science and Engineering

,

Merging Versatile Polymer Chemistry with Multifunctional Nanoparticles: An Overview of Crosslinkable Aromatic Polyester Matrix Nanocomposites

Mete Bakir[a,c], Jacob L. Meyer[a,d], Siyuan Pang[a], James Economy[b,d], Iwona Jasiuk[a,*]

a) Department of Mechanical Science and Engineering, University of Illinois at Urbana-Champaign, Urbana, IL 61801, USA.

b) Department of Materials Science and Engineering, University of Illinois at Urbana-Champaign, Urbana, IL 61801, USA.

c) Digital Materials LLC, Chicago, IL 60607, USA

d) ATSP Innovations, Champaign, IL 61820, USA.

* Correspondence to Iwona Jasiuk. Email: ijasiuk@illinois.edu

Telephone Number: +1-217-333-92-59

,

ABSTRACT

The current trend in the global advanced material market is expeditiously shifting towards more lightweight, multifunctional configurations, considering very recent developments in electrical aircrafts, biomedical devices, and autonomous automobiles. Hence, the development of novel polymer nanocomposite materials is critical to advancing the current state-of-the-art of structural material technologies to address the pressing performance demands. Aiming at expanding the existing material design space, we have investigated crosslinkable aromatic polyesters matrix nanocomposites. The aromatic polyesters, within the thermosetting form, are a prospective high-performance/high-temperature polymer technology, which is on par with conventional epoxy-derivative resins and high-performance engineering thermoplastics in the range of their potential applications. The aromatic matrix-based thermosetting nanocomposites manifest greatly enhanced physical properties enabled by chemistry-favored robust interfacial covalent coupling mechanism developed during the in-situ polymerization reaction with various nanofiller particle configurations. Here, we provide a summary review of our recent efforts in developing this novel polymer nanocomposite material system. We highlight the chemical strategy, fabrication approach, and processing techniques developed to obtain various nanocomposite representations for structural, electrical, optical, biomedical, and tribological applications. The unique characteristic features emerging in the nanocomposite morphologies, along with their physicochemical effects on the multifunctional macroscale properties, are demonstrated. This unique matrix configuration introduces superior performance elements to polymer nanocomposite applications towards designing advanced composite materials.

Keywords: aromatic thermosetting copolyester; high-performance polymers; interfacial conjugation; liquid crystallinity; glass transition temperature.

,

Introduction

Over the last two decades, fundamental and applied research efforts have been devoted to understanding polymer nanocomposite materials. Of particular concern of constructing mission-critical, load-bearing material configurations for aerospace, automotive, and medical applications, polymer nanocomposites demonstrate effectively controllable multifunctional physical properties at macroscale, beyond those of their host polymer matrices.[1] Within this framework, the content of the polymer nanocomposite research has solely been focused on comprehending particular roles of various resin types (e.g., thermoplastics, thermosets) and nanoparticle forms (e.g., graphene, carbon nanotube) towards maximizing material performance factors.[2]

Thermoplastic matrix nanocomposite forms have drawn the most interest in the recent literature due in part to relatively broader application range which is presently available for their host thermoplastic matrices.[3-5] Among standard thermoplastics, also known as commodity plastics, polymethyl methacrylate (PMMA), polypropylene (PP), and polystyrene (PS) have been subjected to extensive analysis with regard to discerning the functions of changing stereochemical configurations, nanoparticle forms, and processing conditions[6-10]. However, these nanocomposite configurations desperately lack adequate mechanical strength and thermal stability stemming from those base polymers, so they ultimately fail to address high-end performance requirements of structural applications. Alternatively, high-performance thermoplastics, including but not limited to, polyether ether ketone (PEEK), polyetherimide (PEI), and polyphenylene sulfide (PPS), manifest clearly superior performance measures, validated by their extensive applications in those aforementioned product markets[11,12]. Significantly higher melt viscosities at comparatively elevated processing temperature windows of the high-performance thermoplastics, as to the standard thermoplastics, hampers the uniform dispersion of nanoparticles within the embedding

,

matrix, rendering well-known agglomeration issues. Thus, thermoplastic matrix nanocomposite material compositions, including both standard and high-performance grades, have not successfully penetrated the advanced materials market for critical structural applications.

On the other hand, thermosetting resins, unlike thermoplastics, undergo an irreversible crosslinking process by which they overall demonstrate promising thermal and mechanical characteristics to potentially meet the binding performance demands in high-end structural representations. Thermosetting nanocomposites have been shown with epoxy-derivates, polyimide (PI), and polyurethane (PU) resins through easy processability and favorable affinity with heterogeneous nanoparticles, leading to considerably improved physical properties over the neat resin forms[13-16]. The key element that shall come along with the thermosetting nanocomposite material compositions is the accessibility to in-situ polymerization condition in which reinforcing nanoparticles and host polymer chains develop chemical interfacial interaction and bonding mechanisms, prior to and during cure reactions[17]. The formation of unique interpenetrated backbone structures clearly differ from the conventional rheologically percolated nanoparticle domains. Although holding a great promise for the refined application domain, the nanoparticle-endorsed improvements in global physical properties of thermosetting nanocomposite configurations have not fulfilled the performance expectations, which may be attributed to operational limitations incurred by available polymer technologies or ineffective interfacial interaction schemes. Hence, aiming at expanding the design and application spaces of polymer nanocomposites, particularly thermosetting nanocomposites for aerospace applications, the Iwona Jasiuk research group at the University of Illinois at Urbana-Champaign has performed interdisciplinary research, with multiple field experts, within the recent years to develop novel crosslinkable aromatic polyesters nanocomposites.

,

Crosslinkable aromatic polyesters were developed in the James Economy research group at the University of Illinois at Urbana-Champaign in the late 1990s following from earlier work in the development of linear aromatic polyesters.[18-21] They were further progressively improved for tribological, adhesive, and composite applications.[22-26] The polymer system utilizes low cost, easily processable, and simply crosslinkable aromatic copolyester oligomers, which are preferentially capped with either carboxylic acid and acetoxy functionalized oligomer groups to form, upon curing, three-dimensional network high-performance polymer systems (**Figure 1**). The polymer matrix can be conveniently reconfigured into different physical forms, including bulk, foam, coating, and adhesive, owing to the unique macromolecular architecture. As reported in the literature, crosslinked aromatic copolyesters demonstrate promising physical properties including high thermal decomposition temperature (> 450 °C), significant glass transition temperature (> 260 °C), morphology controllable dielectric constant (between 2.5 (foam) and 4.5 (bulk)), outstanding mechanical performance (unfilled compressive strength > 300 MPa with 1.3 g/cm^3 bulk density), and adsorption-driven low moisture uptake (<0.3 wt.%) for structural, load-bearing applications.[18,22,27-29] As well, crosslinked aromatic polyesters offer strong high-temperature adhesive characteristics with a lap shear strength up to 21 MPa at very low bondline thicknesses via solid-state self-bonding between two cured polymer surfaces by means of a class of bond exchange reactions termed interchain transesterification reactions.[20,30,31] Of particular interest, crosslinked aromatic polyesters, with the unique interchain transesterification reactions bonding capacity, can be used to enable sub-micrometer thick bondlines in microelectronic devices.[23,32-35] Furthermore, crosslinked aromatic polyesters are outstanding tribological wear coating materials with a low coefficient of friction (0.17-0.19) and impressive wear resistance from cryogenic to elevated temperatures.[24-26,35,36] Moreover, crosslinked aromatic polyesters manifest immense

,

potential as a matrix material in carbon fiber reinforced composite applications due in part to their intrinsic liquid crystalline nature, superb ablative performance with low limiting oxygen index, and intrinsic self-healing properties provided by the interchain transesterification reactions mechanism.[37,38] As well, recent work shows that the interchain transesterification reaction (ITR) mechanism can be used to achieve a reversible adhesive effect on crosslinked aromatic polyester-coated surfaces.[39] These prior studies highlighted several superior performance characteristics of the crosslinked aromatic polyester system to be further explored in high-performance nanocomposite applications.

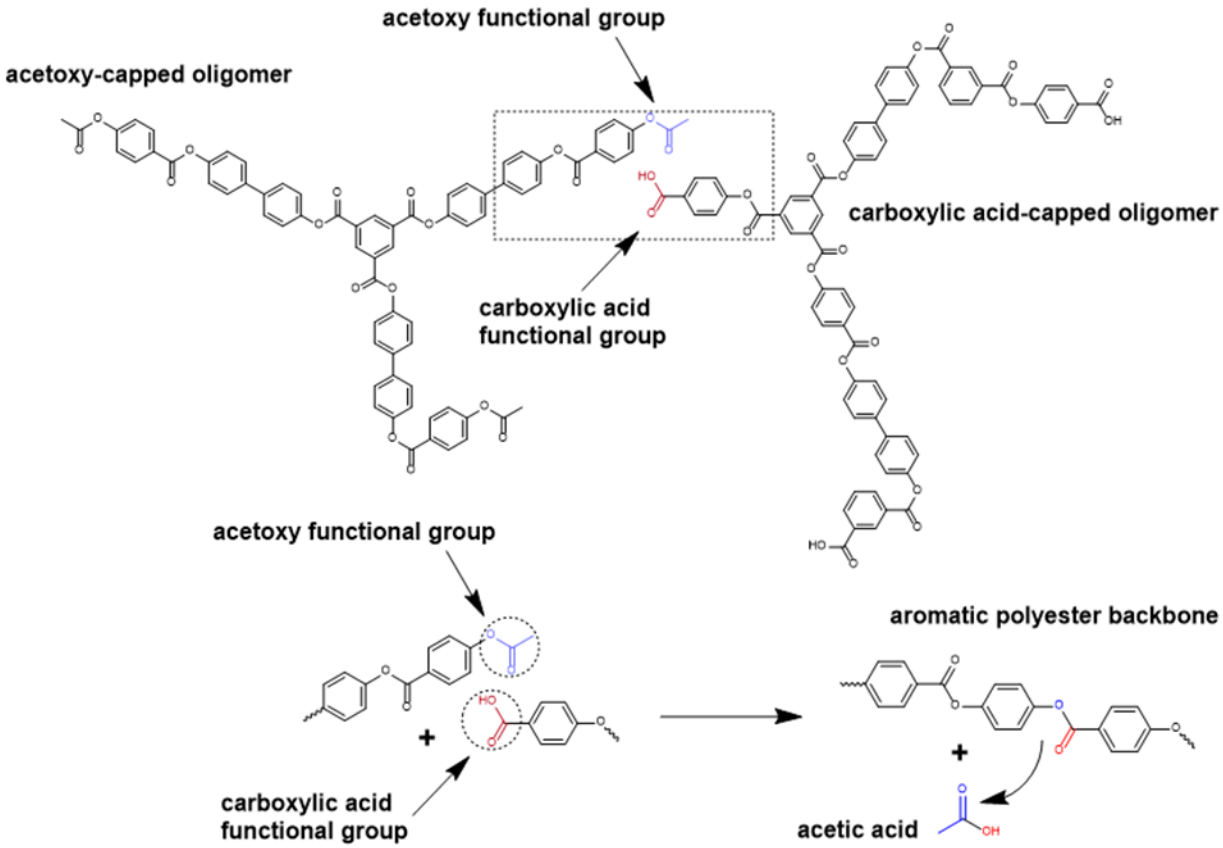

Figure 1. (Top) Representation of typical acetoxy-capped and carboxylic acid-capped crosslinkable aromatic polyester oligomers. (Bottom) Chemical representation of the thermal condensation polymerization reaction mechanism between the constituent acetoxy and carboxylic acid group oligomers generating the crosslinked network of aromatic polyester backbone and discharging acetic acid by-product.

,

All-aromatic thermosetting copolyester are prepared using a set of carboxylic acid-capped and acetoxy-capped oligomers.[18,22] These two oligomer groups are synthesized using different molar ratios of hydroquinone diacetate (HQDA), biphenol diacetate (BPDA), p-acetoxybenzoic acid (ABA), isophthalic acid (IPA), and trimesic acid (TMA) as key building blocks. The heat-induced condensation polymerization reaction is enabled through mixing the two oligomer sets at particular weight ratios in solid-state and carrying out a rationally designed thermal cure process. The polycondensation reaction generates the crosslinked aromatic polyester backbone of the matrix while releasing acetic acid as a reaction by-product. The proposed reaction mechanism is shown in **Figure 2** below. The crosslinked aromatic polyesters can be produced in either amorphous or liquid crystalline formulations by selection of appropriate monomer feed ratio to select crosslink density.[19] Oligomers which do not display birefringence individually in their melt form amorphous polymers when cured while those that do display birefringence produce polymers which are birefringent after full curing – which is also seen in cyanate ester-based oligomers.[29,37,40] Birefringent oligomers have similar molecular weights as isotropic oligomers but with a lower feed ratio of the crosslinker (TMA), which results in a longer chain length between crosslinks.

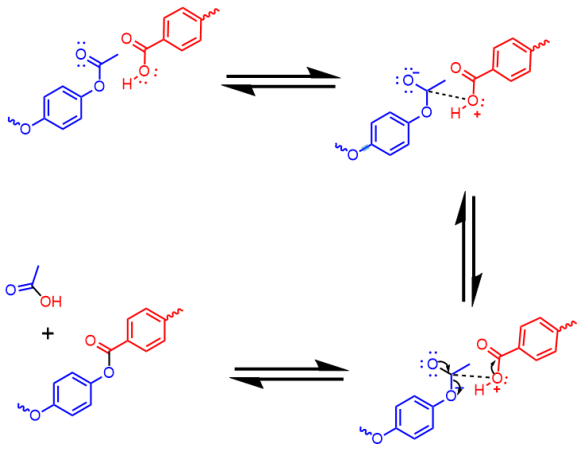

Figure 2. A detailed proposed reaction schematic for cure of crosslinkable aromatic copolyester oligomers. Components in red represents an end-group from a carbolxylic acid-capped oligomer while those in blue represent end groups from an acetoxy-capped oligomer.

,

Heat-Induced Condensation Polymerization Reaction

Building on the prior studies on interchain transesterification reactions, we initially devised a unique chemical strategy to develop self-generated foams.[41] Low-cost, conventional polymer foams find extensive use in automobile, packaging, and construction industries by low structural densities, good thermal insulation, and superior acoustic properties[42,43]. Yet, the state-of-art polymer foam compositions show relatively poor strength-to-weight ratio and low thermomechanical stability, which overall limited their implementation into high-performance applications. On the other hand, due in part to the current interests in lightweight materials, naturally occurring cellular materials can potentially bring more flexibility into material development processes to deliberately tailor final physical properties towards target performance needs. Aromatic thermosetting polymer foams realize the aforementioned superior physical properties of the crosslinked polyester resin within low-density three-dimensionally porous morphology. The facile thermosetting foam fabrication method utilized rationally designed aromatic based carboxylic acid- and acetoxy-capped constituent oligomer groups to perform a heat-induced condensation polymerization reaction with a self-released blowing agent generating macrocellular foam structures.

As shown in **Figures 1-2**, the polymerization reaction mechanism is an acidolysis-type interchange condensation reaction, which can also be classed as a transesterification. During the polycondensation process, the hydroxyl group of the carboxylic acid functional group is replaced by the ether oxygen of the acetoxy functional group which established the crosslinked ester backbone of the crosslinked aromatic polyester matrix while releasing acetic acid as the reaction

,

by-product.[29,44] The constituent oligomers are synthesized from a set of benzene derivative monomers, which are connected together via covalent oxygen bonds. Hence, the chemical backbone structures of the oligomer groups are successfully retained during the polymerization reaction owing to high thermal stability and chemical inertness of the aromatic rings, intramolecular cohesive binding energies of oxygen bonds, and their comparable electronegativities. Consequently, only chemically reactive acetoxy and carboxylic acid functional groups participate in the condensation polymerization reaction releasing acetic acid as the main product of the reaction. The acetic acid appears in the gas form in the molten oligomer medium in the course of the polymerization process as the corresponding reaction temperatures exceed its boiling point of ~118°C. As a result, the acetic acid by-product behaves as a convenient internal blowing agent that generated a three-dimensionally porous polymer matrix.

Xu and Economy studied pore formation using a variety of condensation by-products during the curing of crosslinkable aromatic copolyester oligomers.[45] Aliphatic acid by-products were introduced into the oligomers by reacting the fully cured resin with corresponding aliphatic acids. This two-step foaming process was utilized to study the effects of the boiling point of the by-product on foaming under controlled atmospheric pressure. It was found choosing a by-product with a boiling point higher than the curing temperatures, finer pores (down to a range of 0.5-1.5 μm) could be generated, but the use of these by-products did not produce a decent homogeneity in the Z-axis for thicker specimens. Those results were in line with Frich and Carter on species found in the collected by-product when using acetic acid as the foaming agent.[19,46] A low concentration of hydroquinone diacetate (a feed monomer used in the synthesis of a carboxylic acid capped oligomer) was observed via nuclear magnetic resonance (NMR) due to the low sublimation temperature (121°C) comparable to the boiling point of acetic acid (122°C). It was also found that

,

low boiling point constituent monomers were at risk of leaving the system due to random exchange via ITR, sometimes resulting in monomers effectively being scissioned from the polymer bulk.[45] This effect is suppressed with increasing boiling point and reduced sublimation pressure of constituent monomers. Later substitution of hydroquonine diacetate to biphenol diacetate effectively suppressed the presence of undesired ITR-sublimate derived by-product.

The foaming reaction reveals fundamental phase transformation stages developed during the heat-induced condensation polymerization reaction between the functionally-capped oligomer groups (**Figure 3**). Starting with mixing the constituent oligomer powder particles in solid-state, the heat-induced melting characteristics, bubbling processes, and cure formations are both visually and analytically studied for high crosslink density/low molecular weight and low crosslink density/high molecular weight grades of aromatic thermosetting foams. High crosslink density/low molecular weights grade oligomers undergo the phase transformation stages at relatively lower temperatures, which also yield bubble nucleation at higher rates. The crosslinked aromatic polyester foam yield a glass transition temperature as high as 191°C, along with thermal degradation stability temperature above 500°C. Linear thermal expansion of the foam is as low as 1.2% at 200°C. Furthermore, the foams deliver a robust structure for which compressive mechanical strength is measured to be around 10 MPa with 0.63Mg/m^3 density (or 0.48 relative density). All results are confirmed by the above mentioned earlier studies. The novel aromatic thermosetting foam configuration populate a new design space to deliver multifunctional properties with deliberately controllable lightweight, yet robust morphologies, as of fully dense polymeric materials, along with extraordinary thermal performance profiles for critical, primary load-carrying structural parts exposed to elevated operating temperatures.

,

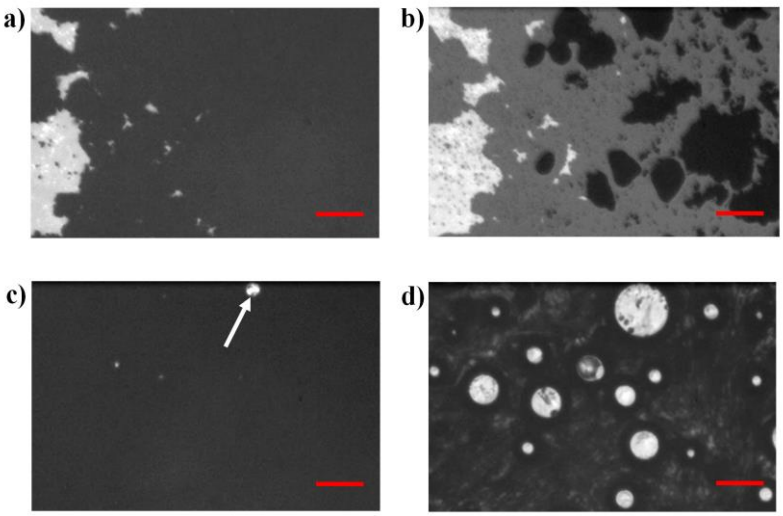

Figure 3. Phase transformations during the foaming process of (a) curing polymer at 30°C, (b) melting starts at 180°C, (c) reaction by-product acetic acid releases nucleating bubbles at 230°C, (d) cross-linking formation and bubble growth at 270°C. The scale bar is 5 mm.[41]

Our initial study helped us to understand the characteristics of the chemical reaction as well as determine the base physical properties of the crosslinked aromatic polyester foam structures before introducing any nanofiller particles. In that study, one of the particular performance measures that we observed was the significant mechanical strength for such a low-density foam structure, indicating promising material toughness. To further explore this feature for impact energy absorption cases, we then adapted the very same chemical methodology to fabricate composite sandwich materials.[47] For energy absorption and impact resistance applications, aluminum foam can sustain high strain rate large plastic deformations to convert kinetic impact energy into plastic deformation energy.[48] Within this scope, polymer foams also have energy absorption capacity to minimize the impact load transmitted through them.[49] The standard polymer foams lack mechanical strength to survive the localized impact effects. Alternatively, sandwich layered multimaterial configurations demonstrate the optimized performance, yet currently suffer from weak interlaminar adhesives, ultimately resulting in delamination.[50] The crosslinked aromatic polyester foam core is synthesized between the aluminum foam face layers via the

,

thermal polycondensation reaction.[47] The crosslinked aromatic polyester foam core strongly adheres to the face layers facilitated by *in situ* attraction mechanism between surface hydroxyls of the aluminum and polar ester bonds of the constituent oligomers.[30,32] Lap shear experiments demonstrate that the interfacial bonding strength is superior to the tensile performance of the bare aluminum foam parts (~ 1.2 MPa). The composite sandwich structures yield excellent absorption performance. Drop-weight impact tests show that the three-layer sandwich structure absorbed four times the impact energy as compared to the bare aluminum foam of the same overall thickness. We conclude that the robust interlaminar bonding along with strong mechanical properties of the crosslinked aromatic polyester foam promoted the enhanced impact energy absorption performance (with 200 J-cm^3/g of energy absorption density) of the sandwich composite structures. Note that the crosslinked polyester foam cores develop robust interfacial bonding during heat-induced cure process with high-performance aluminum and titanium alloys, stainless steel, and high-temperature polymer composite laminae. Thus, the demonstrated sandwich composite configuration can find use in structural, ballistic, crash impact energy absorption applications.

Near-Homogenous Nanofiller Blending with Solid-State Mixing Approach

Our primary work on the crosslinked aromatic polyester nanocomposites demonstrated the development of carbonaceous nanoparticles incorporated nanocomposite foams.[51] In addition to the energy absorption and impact resistance applications, polymer foams can potentially fulfill the need for space-filling, strong, and lightweight structural materials, along with acoustic damping characteristics.[52] Nanocomposite foam configurations have demonstrated significant improvements over the thermophysical properties of neat polymers, thus constitute a promising strategy to overcome the performance limitations dictated by the host matrices. Besides,

,

multifunctional features of nanocomposite foams have enabled further interdisciplinary studies on thermal insulation, electromagnetic shielding interference, and acoustic damping.[53-55] However, the contemporary polymer nanocomposite foam configurations fall short of the operational performance requirements caused either by modest physical properties of host polymer matrices or nanofiller-averse processing techniques. The conventional liquid-phase shear-mixing based methods can only deliver broken nanofillers or aggregated nanofiller regions, which limits the performance enhancements to be translated from the nanofillers to the nanocomposite matrix.[56] In our study, a solid-state mixing based, "nanofiller-friendly" fabrication method is introduced to enable near-homogenous combinations of the precursor oligomers with carbon nanofillers (including graphene nanoplatelet (GNP), carbon nanotube (CNT), and carbon black (CB) at individually constant 3 wt.% loading ratio) in powder form prior to the polymerization process (**Figure 4**). That method, which addresses the troublesome nanocomposite processing issues, establishes geometrical conformity between the oligomer particles and nanoparticles, both having micron-scale features, which results in the formation of additional short-range attractive interaction forces. Due in part to the interparticle forces coming into effect, the van der Waals forces between the individual nanoparticles, that frequently impede effective dispersion, are substantially mitigated.[57] Hence, the physical separation of the nanoparticles is facilitated during the mixing process, and phenomena of agglomeration are thereby suppressed. That method also generates a "soft-bed" for the nanofiller particles, which helps to preserve the pristine as-produced geometrical configurations of the nanoparticles, on the contrary of aggressive shear mixing based approaches.[58,59] Furthermore, during the polymerization reactions of nanocomposite compositions, the gaseous acetic acid emission into the molten oligomer medium generates hydrodynamic motion which causes the relocation of the blowing agent bubbles.[60] Such an intrinsic blending

,

mechanism is utilized to process nanocomposites with enhanced the redistribution and rearrangement of the nanofiller particles during the polymerization process. As well, the cure regions show slightly broader temperature windows as well as stronger endothermic nature than the parent material without nanofiller additions, indicating interfacial grafting within the molten medium that alters viscous characteristics. Regardless, the analytic analyses of post-cure characteristics indicate sufficiently cured conditions. All combined, *in situ* synthesized crosslinked aromatic polyester nanocomposite foams, wherein the carbonaceous nanofillers and constituent oligomer groups are concurrently present, display significant physical property improvements. As compared to their base form, the nanocomposite foams show a reduced coefficient of thermal expansion by 25%, wherein above highlighted interfacial entanglements with nanofillers arguably alter the chain relaxation characteristics. Thermal stability (as determined by the temperature at 5% mass loss) is increased by 30°C. The improvement in the thermal stability is attributed to the effect of carbonaceous nanofillers being thermal barriers to shelter the polymer backbone structure from thermal effects and slowing down the bond scissions. Compressive mechanical strength is improved two-fold along with a nearly doubled fracture strain, which ultimately enhances the material toughness by two-fold and generates more damage-tolerant morphology. The results on the mechanical characteristics highlight that the nanocomposite foams uniquely show simultaneous increases in the strength and the maximum strain, meaning improved material toughness, delivering more deformation-tolerant morphologies.

,

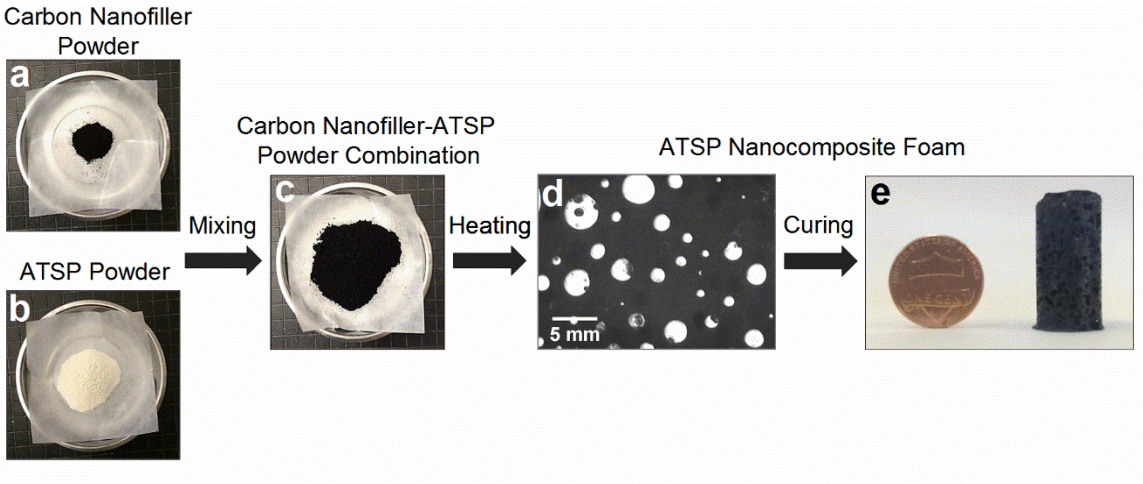

Figure 4. Carbon nanofiller powder, uncured aromatic polyester powder (mixture of precursor oligomers), carbon nanofiller- uncured aromatic polyester powder combination, uncured aromatic polyester-GNP combination subjected to the thermal polymerization reaction at 290°C, and a fabricated crosslinked aromatic polyester nanocomposite foam.[51]

In addition to the significance of the mechanical properties, polymer nanocomposites doped with electrically conductive carbonaceous nanofillers are promising for emerging energy storage and electromagnetic interference shielding applications. Particularly, the formation of interconnected conductive nanofiller networks, also known as a percolation threshold, within intrinsically insulating polymer domains, is imperative to control the electrical characteristics of the nanocomposites. Hence, the scope of the following work is to study the electrical conductivity performance of crosslinked aromatic polyester nanocomposites. Specifically, the physicochemical effects induced by GNPs of different sizes on the condensation polymerization reaction through the formation of percolating networks are investigated.[61] The controlled GNP size incorporated into the crosslinked aromatic polyester matrix forms different electrical percolation thresholds and ultimate electrical conductivities (**Figure 5**). In particular, GNP 1 μm shows the conductive percolating network around 5 wt.% while GNP 5μm and GNP 25 μm display the interconnected domains near 4 wt.% and 3 wt.%, respectively.[62] The ultimate electrical conductivities at 10 wt.% of the nanofiller particles were observed to be on the orders of 10^{-3} S/m for GNP 1 μm, 10^{1} S/m

,

for GNP 5 μm, and 10^3 S/m for GNP 25 μm. The larger GNPs readily formed clusters through the electrical percolation formation in which the nanofiller particles interacted with the matrix and yielded considerably modified topological features along with increased structural densities.[63] Due in part to the strong intermolecular affinity between the GNPs and crosslinked aromatic polyester matrix, a fraction of the reactive functional groups of the constituent oligomers interacted with the GNP particles which resulted in the reduced oligomer fraction participated in the polymerization reaction. The underlying *in situ* interaction mechanism arise due to intermolecular attraction forces between highly polar acetoxy and carboxylic acid reactive groups of the oligomers and inherently oxygen-bearing polar sites on the GNP particles.[64] Initially, molten oligomer domains at elevated temperatures blend and wet the carbonaceous nanoparticle surfaces by means of hydrodynamic forces coming into effect by the acetic acid by-product release. This process facilitates the polar force induced interfacial interactions between the reinforcing nanoparticles and the host matrix. The oligomers containing acetoxy and carboxylic acid functional sites crosslink with the oxygen-beating polar sites on the carbonaceous nanoparticles. In the meantime, the heat-induced cure process robustly tethers the nanoparticles to the forming crosslinked network. It is worthwhile to mention that during the cure process, only a fraction of the functional reactive sites on the oligomers participate in the interfacial attachment process, so nanofiller content beyond the electrical percolation threshold level impedes the completion of regular esterification process. Consequently, caused by increased molten oligomer domain viscosity along with robust interfacial grafting, thermochemical changes also occur in the acetic acid evolution schedule during the polymerization process.[65] Ultimately, higher density foam morphologies are obtained concerning incremented nanofiller loading content. Also, as noted above, vitrification induces slower cure rates wherein the cure reaction becomes more diffusion-controlled rather than kinetic controlled,

,

which also correlates to the cure region temperature broadening. The understanding of physicochemical effects induced by the nanofiller particles of different sizes on polymerization reaction helps to control the formation of electrically conductive percolating networks.

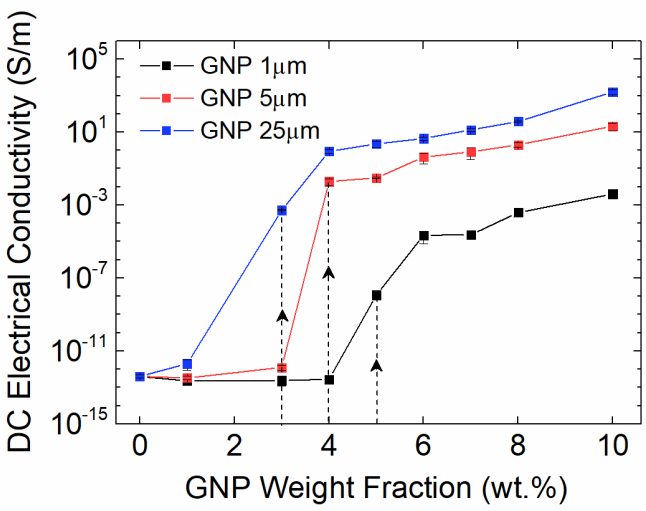

Figure 5. DC electrical conductivity measurements on the crosslinked aromatic polyester-GNP nanocomposites incorporating GNPs of 1 μm, 5 μm, and 25 μm sizes. Standard deviations were represented with error bars. Dashed lines indicate assigned percolation thresholds for corresponding GNP size.[61]

Covalently Conjugated Crosslinked Nanocomposite Network

The aromatic polyesters are thermotropic liquid crystalline polymers. Liquid crystalline polymers offer unique interfacial compatibility with carbonaceous reinforcements within structural composite materials with high-performance properties. For example, p-acetoxybenzoic acid/diacetoxy hydroquinone based thermotropic liquid crystalline polymers, particularly amorphous form of crosslinked aromatic polyesters with phenyl ester groups, develop covalently conjugated mesophase domains around reinforcing carbon fibers.[66,67] Liquid crystalline resins are likewise compatible with nanofiller particles that result in notable improvements in macroscopic physical properties, such as mechanical toughness and electrical conductivity.[68,69] To realize this unique physicochemical phenomenon in composite applications, the thermally induced phase transition characteristics, along with the effects of nanofiller particles on polymer matrix chain

,

relaxation characteristics, shall be the focal point of ongoing research efforts. Along with that line, we characterized the interfacial interactions between carbonaceous nanofillers and liquid crystalline grade crosslinked aromatic polyester on the physical properties of nanocomposite structures. We show the formation process of preferentially oriented interfacial liquid crystalline mesophase domain around GNP particles within an amorphous aromatic thermosetting copolyester matrix.[70] A nematic phase liquid crystalline network develops at the nanoparticle and matrix interface via the crystalline carbonaceous structure induced local ordering effects upon completion of the thermal cure process (**Figure 6**).[37,66,67] The liquid crystalline phase contour mirrors the shape of GNP domain owing to the surface-induced ordering mechanism. Birefringence patterns observed in the interface region around GNPs are visualized in sharp contrast to the surrounding matrix. The liquid crystalline region demonstrates a thermally reversible phase transition characteristic such that isotropic morphology (appeared with visual uniformity to the surrounding matrix) was obtained through a heating cycle, which reversed back to the nematic form following a subsequent cooling cycle.[71] Also, the glass transition characteristics of the liquid crystalline crosslinked aromatic polyester-GNP nanocomposites are studied. The nanocomposites show glass transition temperatures of 220 °C and 227 °C with 1 wt. % GNP and 5 wt. % GNP, respectively. The glass transition temperature of the neat matrix is 214 °C. The corresponding increases in the glass transition temperature occur due to the robust coupling of GNPs to the crosslinked aromatic polyester matrix through the liquid crystalline network, as verified through solid-state nuclear magnetic resonance analysis. The rigid-core mesogen units introduce an additional intermolecular stiffening to the system as the polymer matrix underwent structural relaxation during the phase transition. Hence, the liquid crystalline interphase causes restricted chain mobility within the crosslinked network of the crosslinked aromatic polyester nanocomposite matrix which resulted

,

in upshifted glass transition temperatures.[72] Through such a unique liquid crystalline interlayer formed around the graphene nanoparticles, this robust interfacial attachment scheme can help to enhance the overall thermophysical properties of nanocomposites of particular interests.

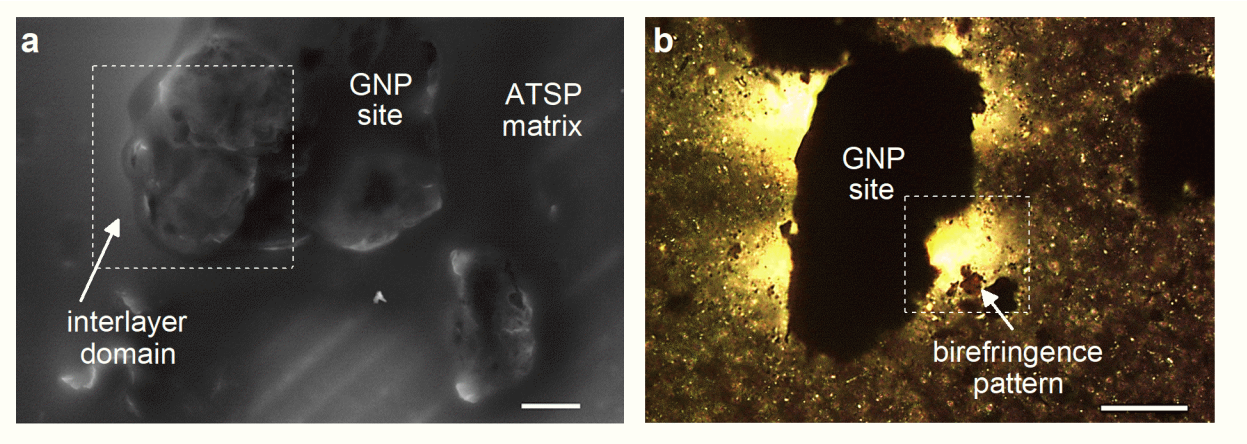

Figure 6. Scanning electron microscopy image of the interlayer LC mesophase domain (darker) around a graphene nanoplatelet particle aggregation site in crosslinked amorphous aromatic polyester matrix (brighter) (a). Cross-polarized optical microscopy image of the birefringence patterns (brighter) radiating from an individual graphene nanoplatelet particle (darker). The scale bars are 20μm.[70]

To further explore the interfacial coupling between crosslinked aromatic polyester matrix and GNP nanofillers, we performed a comprehensive analysis on the glass transition (Tg) characteristics of nanocomposites with amorphous grade crosslinked aromatic polyester.[73] Aiming at maximizing macroscale physical properties, a primary research thrust on polymer nanocomposites has been directed on efforts to realize robust interfacial coupling mechanisms between nanofiller particles and polymer matrix chains. To date, edge-or-surface-functionalized nanoparticles have been demonstrated to develop covalent bonding with both thermoplastic and thermosetting polymers, causing shifts in glass transition temperatures.[74-77] In this line, the glass transition temperature shifts are also controlled by the backbone architectures wherein the aforementioned interfacial bondings occur through relatively weak intermolecular attachment schemes. As a result, the state-of-the art polymer nanocomposite configurations have not been proven with robust interfacial coupling mechanisms to ultimately optimize macroscale physical

,

properties. In that study, nanofiller-contiguous polymer network with aromatic thermosetting copolyester nanocomposites is presented in which carbon nanofillers covalently conjugated with cure advancing crosslinked backbone chains through functional end-groups of constituent precursor oligomers upon an *in situ* polymerization reaction. *In situ* synthesized neat crosslinked aromatic polyester foam base material, having amorphous morphology, displays a sub-glass transition at 79 °C and glass transition at 191 °C. Correspondingly, the nanocomposite structures, individually incorporating GNP, CNT, and CB nanofiller particles, yield positive shifts in the Tg peak positions by around 80 °C along with broadened glass transition peaks having breadth baselines widened approximately 100 °C (**Figure 7**). As well, the sub-glass transition peak of the nanocomposite morphologies is suppressed. On the other hand, a mixture of pre-polymerized crosslinked aromatic polyester formulation with the GNP particles (while GNPs are not present during the initial polymerization process) does not produce any deviations in the Tg peak position. It is concluded that the nanofiller particles behave as crosslinking agents during the polymerization reaction such that the nanoparticles effectively join the highly-crosslinked network of the crosslinked aromatic polyester matrix. The functionalized oligomers interact with oxygen-bearing polar sites inherently present on the GNP particles that conjugate the nanoparticles to the advancing crosslinked network of the crosslinked aromatic polyester backbone network. Following the GNP particles joining to the crosslinked network of the backbone, the nanocomposite form a nanofiller-contiguous morphology in which macroscopic thermomechanical behaviors of the nanocomposites are substantially altered by the orders of magnitude higher in-plane elastic properties of the GNP nanoparticles. The nanofiller-contiguous network displays a thoroughly modified relaxation behavior for the backbone chain, rather than imposing a physical confinement effect, which hence reflect the macroscale response of the

,

nanocomposite structure. In the glass transition region, the nanofiller particles, while strongly tethered the polymer backbone, induce a pseudo-rheological percolation behavior facilitated through short inter nanoparticle distances, which restricts the mobility of wide-extending long chains, increasing the overall chain relaxation time.[75,76] The pseudo-rheological percolation applies to a crosslinked thermoset polymer network wherein conjugated nanofiller particles generated a "local jamming effect" over junction points to polymer chains during the relaxation process. Note that the high-temperature stability of the nanofiller-conjugated oxygen bonds of the functional groups of the oligomers enables the broadening effect at elevated temperatures, which hence differs from the marginal temperature shifts enabled via relatively weaker coupling schemes discussed above. The glass transition temperature trends, along with the strong interfacial attachment schemes, extend beyond the contemporary polymer nanocomposites that shall potentially lead to further studies to explore the effects in multifunctional properties.

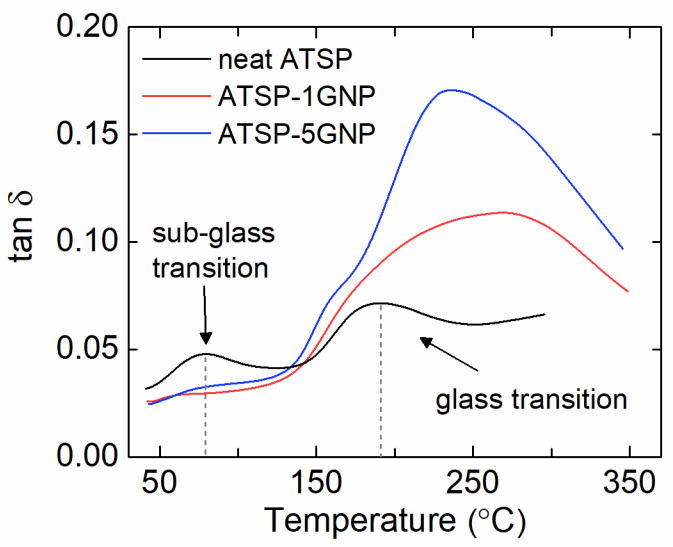

Figure 7. Dynamic mechanical analysis tangent delta measurements of the *in situ* synthesized foam morphology nanocomposites with graphene nanoplatelets. Nanocomposites were named by weight fractions of the added nanofillers (1 wt % and 5 wt %).[73]

,

Three reaction mechanisms are proposed for interfacial reactions between the crosslinkable aromatic copolyester oligomer melts and the carbonaceous nanofiller particles. Several pieces of information are important to this consideration: 1) non-ester functional groups from the aromatic copolyesters are found to generally disappear completely after cure along with observable functional from the carbon nanofillers as seen in solid-state NMR – therefore mechanisms, where functional groups are consumed to produce ester linkages, should be included; 2) no modification to the glass transition is observed in experiments between nanofiller added to fully cured resins rather than reactive crosslinkable oligomers; 3) reactions are deduced to principally be between oxygen-bearing components of the crosslinkable aromatic copolyester oligomers and the nanofiller. The first proposed reaction type is between the acetoxy-capped oligomers and carboxylic acids found on the nanofiller surfaces. This reaction proceeds by nucleophic addition wherein an acyl oxygen on a carboxylic acid adds to a carbonyl of an acetoxy end-cap.[78] The tetrahedral intermediate of the original polyester acyl oxygen eliminates an ester linkage formed between the original ester oxygen and the carbonyl of the nanofiller carboxylic acid. This also produces acetic acid as a by-product, as seen in **Figure 8.a**. An example of using this class of reaction is the reaction of polyethylene terephthalate (PET) with 4-acetoxybenzoic acid (4-ABA) to produce a copolymer.[79] This reaction increases the degree of cure of the resin, unlike the other proposed mechanisms. The second reaction mechanism, as shown in **Figure 8.b**, is formally similar to the transesterification cure seen above with the modification that the degree of cure does not strictly change, and an aromatic carboxylic acid is produced rather than acetic acid. This reaction pathway would likely require subsequent reaction with an acetoxy functional group within the resin to produce the carboxylic acid-free conditions seen via solid-state NMR. The third type is an exchange reaction between a hydroxyl end group with a neighboring ester that is termed an

,

alcoholysis reaction and is shown in **Figure 8.c**.[80] This reaction proceeds by nucleophilic addition of the hydroxyl to a carbonyl group of an ester linkage. This induces a positive charge to the hydroxyl oxygen and a negative charge to the carbonyl oxygen. The intermediate structure expels an alcohol via electron transfer from the negatively-charged oxygen, which captures a proton from the original hydroxyl. The final result is that exchange occurs at the carbon-oxygen single bond in the original ester.[78] This reaction would require subsequent esterification between the produced aromatic alcohol and a carboxylic acid-capped oligomer to produce the end-group free conditions observed in the produced nanocomposites.

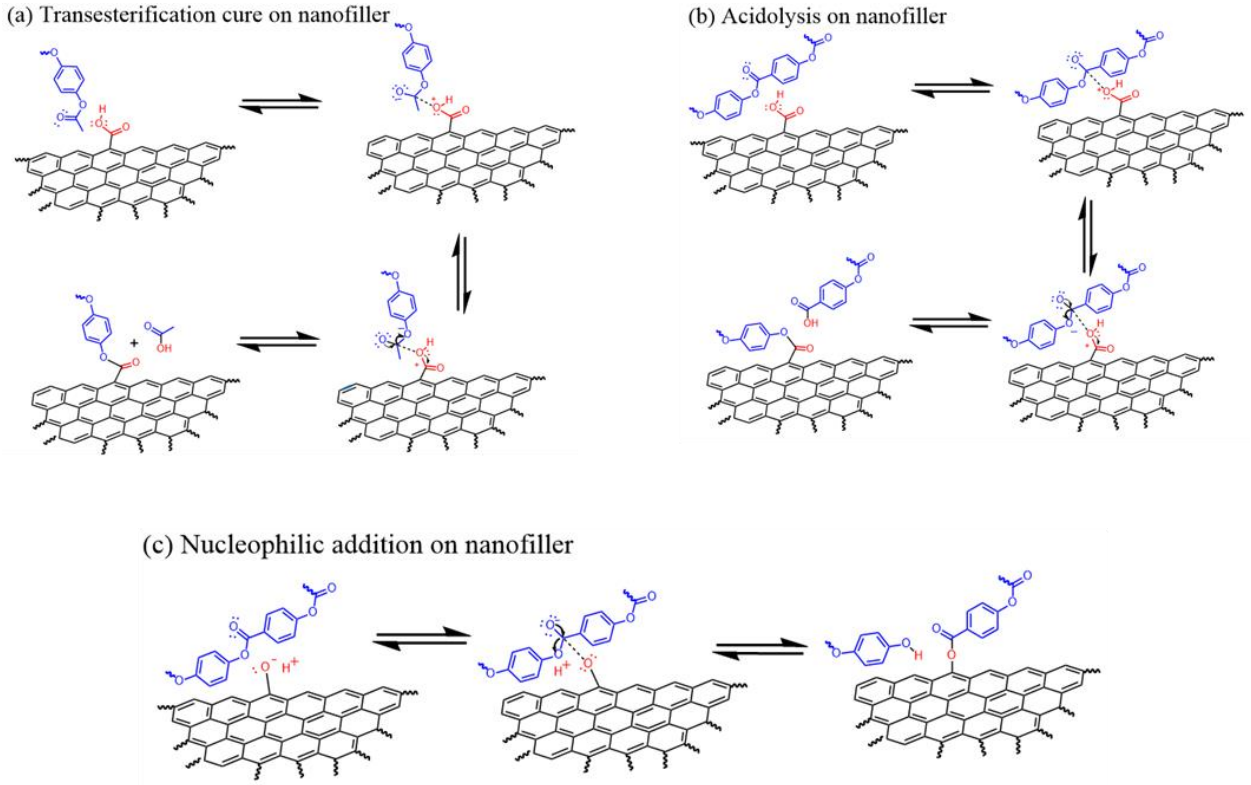

Figure 8. Proposed reaction schemes of crosslinkable aromatic polyester oligomers with carbon nanofillers. **a)** transesterification cure on nanofiller between acetoxy functional groups within the resin melt and carboxylic acid from the nanofiller surface, **b)** acidolysis-type transesterification on nanofiller between an ester linkage from the resin melt and carboxylic acid from the nanofiller surface, **c)** nucleophilic addition on nanofiller between ester linkage from the resin melt and hydroxyl present on nanofiller surface.

,

Lastly, on the GNP nanofiller incorporated nanocomposites, we investigated the effects of environmental aging on the neat and GNP combined nanocomposite crosslinked aromatic polyester matrix through cyclic water immersion and salt spray tests.[81] Particularly, high-performance/high-temperature polymers demonstrate robust physicochemical stability against severe environmental conditions beyond commodity polymers.[82] Owing to their outstanding thermal degradation stability, high glass transition temperatures, and superior mechanical performance, high-performance/high-temperature polymers have found uses in a wide array of applications spanning coatings, composite matrices, fibers, foams, and membranes.[73-86] These polymer configurations are required to sustain superb degradation stability through chemical inertness and low moisture absorption in aqueous solutions towards longer service lives to expand the application space. Our study highlights the long-term aging resistant characteristics of nanocomposites with the crosslinked aromatic polyester matrix. The matrix demonstrates an adsorption-driven mass uptake mechanism owing to having a highly crosslinked morphology that conceivably restricted chain mobility and resulted in reduced diffusion rates.[87,88] Also, a fully cured and highly crosslinked network of the aromatic polyester morphology accommodated the minimum number of polar in the backbone chains by which moisture absorption is also minimized.[89] The crosslinked aromatic polyester nanocomposite had hydrophobic characteristics neutral to the presence of nanoparticles with measured advancing contact angle being around 90°.[90-92] Due to hygroscopic swelling occupying free volumes in the polymer chain structure, an environmental aging caused moderate changes in the glass transition temperature by negative shifts up to 20 °C (depending on testing condition and exposure duration). As well, the thermal degradation stability (within 10-20 °C), as well as the compressive mechanical strength of the crosslinked aromatic polyester morphology, were maintained during the extenuated aging

,

processes.[93] The findings of this study may lead to further efforts over a comparative, systematical study of aging performances of high-performance polymers.

Tailoring Nanocomposite Morphology with Self-Assembly

Referring to the previous arguments on the interfacial coupling mechanism between the crosslinked aromatic polyester matrix and GNP nanofillers, and discussions on the corresponding modifications induced in the material behaviors of nanocomposites, we investigated surface wettability effectiveness of the crosslinked aromatic polyester resin on carbonaceous surface nanofiber system. As previously shown in the literature, the formation of periodically functionalized and crystalline form architectures on matrix-embedded nanostrands through leads to a facile interfacial coupling scheme.[94] The carbon nanostructures form nucleation sites for polymer matrices during the crystallization process. The polymer chains show an epitaxial growth mechanism through a unique lattice match with the carbon-based nanofillers.[95] Particularly, hierarchical shish-kebab structures of inter-and-trans-crystalline configurations are obtained with carbon nanotubes and semicrystalline polymers through size-dependent epitaxial growth schemes.[96-98] We report on *in situ* epitaxial step-growth polymerization reaction driven interfacial functionalization of crosslinked aromatic polyester with multi-layered graphene wrapped alumina nanofiber surface.[99] During the thermal condensation polymerization, crosslinked aromatic polyester dip-coated fiber strands develop a nano-hybrid shish-kebab structure with periodically assembled and off-surface grown micron-scale lamella crosslinked aromatic polyester domains (**Figure 9**). This form of the crosslinked aromatic polyester with fiber structure is akin to the nano-hybrid shish-kebab structures with the fiber strand being “shish” and the crosslinked aromatic polyester lamellae being “kebab”.[100-102] Because of the crystalline epitaxial structural order of the nanofiber surface, the crosslinked aromatic polyester backbone chains conceivably rearrange their

,

configurations, which is enabled through polymer intrinsic flexibility at elevated temperatures. In particular, three major mechanisms are conjectured to stimulate this process: the Plateau–Rayleigh instability, the Marangoni effect, and the epitaxial crystal growth. Initially, the constituent oligomer solution film, especially at the low concentration coating the fiber strands, undergo the Plateau–Rayleigh instability at elevated temperatures during the thermal cure process wherein surface undulations take place, causing nucleation sites to be periodically arranged. Next, the Marangoni effect relocates the oligomer molecules as driven by the effective capillary forces on site, concentrating on particular nucleation sites. Then, through the cure reaction, an epitaxial growth mechanism proceeds.[103-105] Thus, inherently amorphous crosslinked aromatic polyester chains form lamellar structures.[106] X-ray diffraction measurements reveal the formation of mesomorphic, preferentially aligned lamella phase which is not present within neither the neat crosslinked aromatic polyester nor pristine fiber samples. Moreover, results of chemical spectroscopy and thermogravimetric analysis highlight the development of an interfacial coupling between the graphene-coated ceramic nanofibers and the crosslinked aromatic polyester matrix. This study lays the groundwork to follow-up studies of aromatic polyesters with nanofiller reinforcements on the *in situ* surface functionalization to generate robust interfacial coupling.

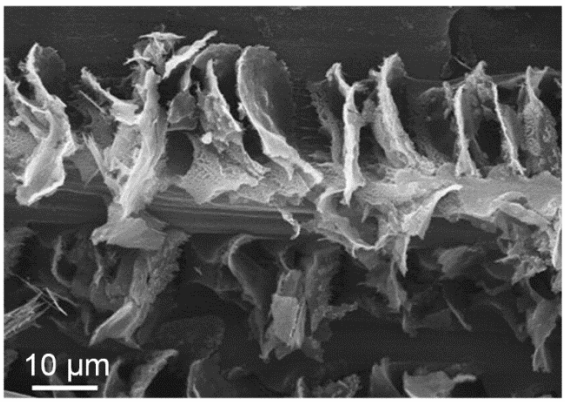

Figure 9. A scanning electron microscopy image showing the formation of the nanohybrid shish– kebab crosslinked aromatic polyester structures on the fiber surface.[99]

,

Of particular interest, building on those above promising structural properties, crosslinked aromatic polyester matrix, in photonic applications, bears high potential to afford ultraviolet (UV) shielding with mitigated photo-degradation and enhanced operational efficiency. The electro-optical properties of the crosslinked aromatic polyesters (e.g., oxidation potential, fluorescence, and band gaps) are local and mediated by isolated aromatic rings.[107] Therefore, doping the aromatic matrix with luminescent nanomaterials can potentially enable high optical activity for applications such as solar energy harvesters, filters, and down converters.[108-111] In that regard, we develop nanocomposites to impart strong photoluminescence within the weak luminescent crosslinked aromatic polyester matrix by incorporating silicon (Si) nanoparticles (Sinps) to obtain luminescent polymer nanocomposites (**Figure 10**).[112] We investigate the polymerization process in solution with the presence of the luminescent Sinps under both UV exposure and thermal treatment. The pre-polymerization combination shows that Sinps did not compromise luminescence when mixed with precursor oligomers. The observed small redshifts in luminescence spectra indicate the interfacial coupling of Sinps to the backbone of the polymer via Si-O bond, which effectively lowers the quantum confinement for radiative recombination of the UV-excited excitons. The unique formation of luminescent oligomer–Sinps complexes in two-dimensional (2D) thin films is observed.[113] Under UV irradiation, the hydrogen bond on the Sinps is cleaved, which turn the particles into reactive charged free radical structures. Sinps can interact with carboxylic acid reactive functional group forming Si-O-C.[114] Alternatively, the charged Sinps can also interact with the double-bond oxygen sites in the C-group oligomer.[115] These two processes result in the formation of a charged complex wherein the oligomer act as a bi-linker. Sinps incorporate within crosslinked aromatic polyester films are transparent in room light, yet they display red luminescence under UV, which is a fingerprint of Sinps (**Figure 10**). With regard to the physical

,

properties, the neat crosslinked aromatic polyester films display a glass transition temperature of around 258 °C, having highly crosslinked and amorphous morphology. In comparison, the Sinps nanocomposite films yield an average glass transition temperature at 259°C. The similar glass transition temperatures and characteristics of neat crosslinked aromatic polyester and Sinps nanocomposite films indicate that Sinps are well incorporated into the crosslinked aromatic polyester matrix. As such, we can infer that the Sinps conjugate with the crosslinked network of crosslinked aromatic polyester while they do not significantly change the network configuration or average molecular chain length.[77]

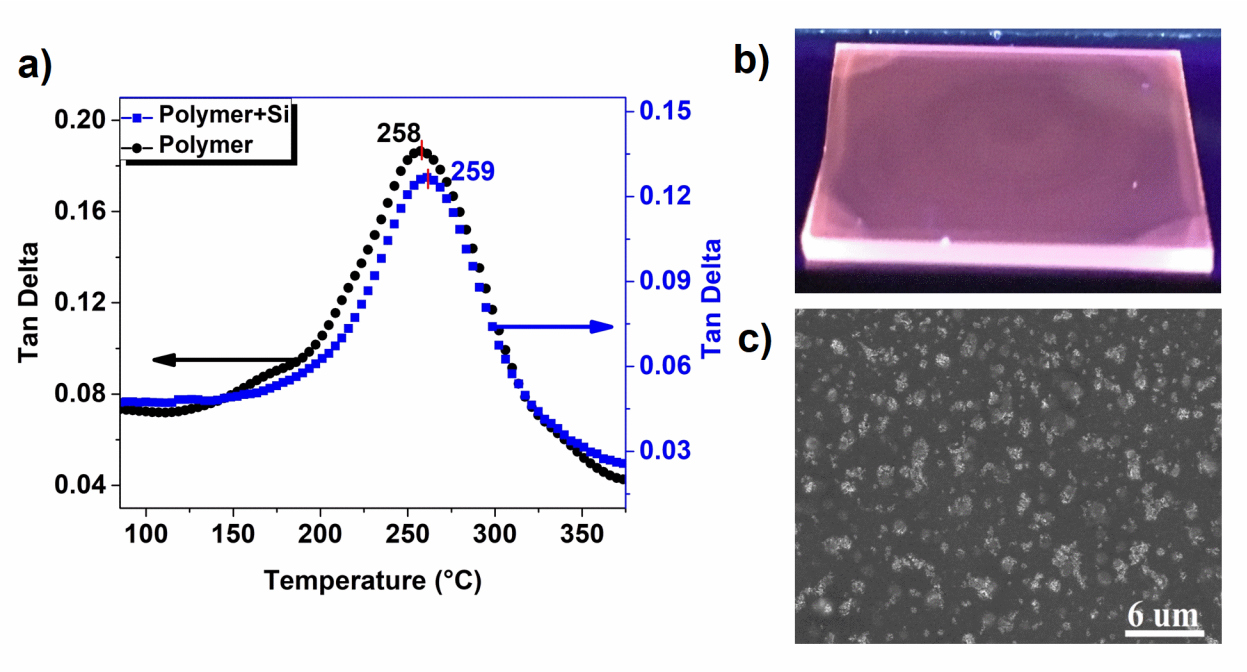

Figure 10. a) Dynamic mechanical analysis of tangent delta glass transition temperatures of neat crosslinked aromatic polyester and Sinps nanocomposite films. **b)** A luminescent image under UV irradiation displaying "red luminescence" in the nanocomposite. **c)** A scanning electron microscope image of the nanocomposite film showing Sinps clusters that varied in size from nearly 50–100nm to several micrometers with an average interspacing of several micrometers.[112]

,

High-Performance Bionanocomposites

Another important application for polymer nanocomposites is the development of synthetic biomaterials. Over the years, polymer bionanocomposites have become the subject of interest in the development of synthetic bone substitutes.[116] Bionanoparticles within nanocomposite matrices serve two purposes: improvement of mechanical properties and enhancement of biological activity for the polymeric domains.[117] Most known biopolymers, including but not limited to poly(lactic acid), poly(glycolic acid), and poly(ε-caprolactone), experience a diffusion-driven hydrolytic decomposition process in *in vivo* conditions.[118] Hence, the permanent implant applications require alternative polymer systems for permanent use (e.g., titanium) in *in vivo* environment. In particular, it remains technically challenging to obtain porous materials consisting of polymer host matrix enriched with bioactive ceramic particles to initiate the reproduction of cellular organisms while maintaining *in vivo* mechanical reliability for synthetic bone substitutes. We present hydroxyapatite (HA) reinforced crosslinked aromatic polyester matrix bionanocomposite as a potential reconfigurable bone replacement material.[119] Earlier work on the crosslinked aromatic polyesters showed direct-contact cytotoxicity test results of fibroblasts remaining healthy and still adhered to the polymer matrix following an incubation period.[120] The morphological analysis demonstrates near-homogenous distributions of the HAs within the matrix wherein both the amorphous nature of crosslinked aromatic polyester matrix is preserved, and HAs are well blended with the matrix in their pristine forms. The HAs behave as a crack-arrester as an intrinsic physical response of the HAs being effectively transmitted to the overall physical response of the nanocomposite structure, which then promotes a more deformation-tolerant formation with relatively enhanced material toughness.[121,122] The compressive mechanical strength is increased by about 10% compared to the parent crosslinked aromatic polyester form. Also, the strain at maximum stress is enhanced by approximately 18% in comparison to the neat structure. Chain

,

relaxation dynamics of the nanocomposite matrix during glass transition is modified via HA-induced segmental immobilization - the nanocomposite exhibit two distinct peaks within the glass transition domain.[122,123] A low-temperature peak arises from the structural relaxation of the matrix (the crosslinked network), which, in fact, slightly downshifts. As well, a high-temperature peak appears due to suppressed segmental relaxation of the chains stemmed from the presence of the HAs. Chemical characterization of the polymer backbone composition reveal the presence of a hydrogen-advanced covalent interfacial coupling mechanism between the HAs and crosslinked aromatic polyester matrix.[124] Future work on aromatic polyester bionanocomposites shall focus on the systematical biocompatibility analysis to lay the groundwork towards designing these materials for various bioapplication schemes.

Nanocomposites for Tribology Applications

Finally, a new area of development is nanocomposite coatings for tribological surfaces for high-temperature applications. While prior studies reported performance improvements through the use of graphene, a recent study by Lan *et al.* demonstrates that the addition of GNPs reduces both the coefficient of friction and wear rate during experiments at 300°C.[125-127] As discussed above, there previously is observation in a related resin of an upshift in the glass transition peak position by 80 °C and a broadening of the peak by 100 °C during dynamic mechanical analysis (DMA) experiments (See **Figure 7**). That particular resin precursor combination is a higher crosslink density and a higher mesogenicity (more rod-like components in the form of biphenol diacetate substituted for hydroquinone diacetate). In the case of an even more closely related resin system with partly similar precursor oligomers, which differ mainly by virtue of a higher crosslink density, a marginal upshift in the peak position of the tan δ is observed with no substantial changes to peak shape.[70] In this case, instead, a marginal drop in the peak Tg, a significant shoulder at 295

,

℃ ,and a sub-Tg peak at 184 ℃ can be observed in **Figure 11**. While observable and substantial changes to the tan δ curve are anticipated for this system, this particular set of changes is not in line with prior observations in the related systems discussed before and likely has origins in the relatively lower crosslink density as compared to the other systems as well as showing reduced mesogenicity. Relating metrics of chain stiffness and crosslink density to observable phenomena in the storage and loss moduli in the crosslinkable aromatic polyesters should be a topic of future study.

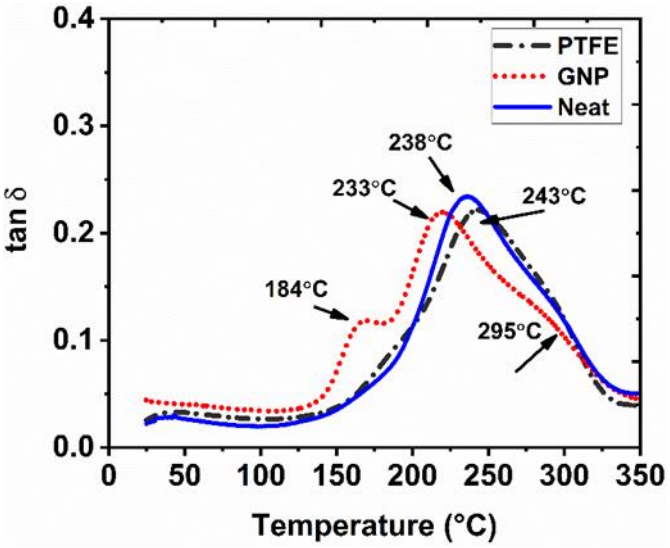

Figure 11. Tangent delta curves by dynamic mechanical analysis for neat, GNP reinforced, and (polytetrafluoroethylene) PTFE blended crosslinked aromatic polyester freestanding films[127].

Conclusion

In conclusion, our preliminary studies demonstrated in this work highlight several key characteristic features of the crosslinked aromatic polyester matrix for high-performance nanocomposite applications. The crosslinked aromatic polyester nanocomposites are prepared via a facile solid-state mixing process by which near-homogenous and intact distribution of nanofiller particles into the polymer matrix is achieved. The precursor oligomers of crosslinked aromatic

,

polyester demonstrate strong chemical compatibility with oxygen-containing nanofiller particles, which establishes a robust interfacial bonding between the backbone chains of the host matrix. Crosslinked aromatic polyester nanocomposites form a nanofiller-conjugated network which significantly alters structural characteristics of backbone chain responses. The crosslinked aromatic polyester nanocomposites exhibit greatly improved physical performance as compared to the neat crosslinked aromatic polyester matrix. Based on the results presented here, the crosslinked aromatic polyester nanocomposites demonstrate an advanced nanocomposite material technology to realize ultimate multifunctional properties to address emerging technological problems. The crosslinked aromatic polyester nanocomposites can find applications in structural engineering materials, energy storage, electromagnetic interference shielding, photonic, and biotechnology applications.

Lightweight and high-performance foam applications are of particular interest for crosslinkable aromatic polyester foams. Owing to superior thermomechanical properties, including glass transition temperature, thermal decomposition temperature, and compressive mechanical strength, the aromatic polyester foams manifest competitive performance measures against counterpart commercial products. The high-performance foam was first devised by NASA in the early 1970s for space environments. Today, two commercial foams are most widely studied and used: Solimide foams and Rohacell foams. High-performance foams are extensively used in aerospace, infrastructure, electronics, transportation, and medicine as flame resistant/retardant materials, impact resistant materials, and thermal/acoustic insulator materials. Polyimide foams, under the trade name of Solimide, is a representative of high-performance foam with low density. Because of its lightweight, low flammability and low smoke characteristics, Solimide foams are used as thermal and acoustic insulation in applications in carbon dioxide removal and compression

,

systems, acoustic barrier, aircraft sidewall and fuselage, ECS systems, cushions, vibration damping materials, marine hull board, expansion and contraction joints, electrical insulation materials in submarines. Formaldehyde-free solimide shows long-term stability (under humid environment and temperature cycling conditions), high ignition resistance, and low flammability properties. These foams can be further densified to meet higher mechanical and thermal requirements for the aircraft application of high-temperature instrument insulation and bleed air duct insulation.[128-132] On the other hand, Solimide foams are limited to low densities and low physical properties, thus have limited applications. A novel closed-cell polyimide foam was developed by NASA Langley Research from the reaction of polyimide precursor residuum. The solid residuum foams can range densities between 8-320 kg/m^3.[133]. The thermogravimetric analysis study revealed that a grade of polyimide foam lost 10% weight at 518°C and lost all of the weight at 580°C, which showed excellent fire resistance properties.[134] Later, a thermally cross-linked polyimide foam with 3,3',4,4'-benzophenone tetracarboxylic dianhydride (α-BTDA), 4,4'-ODA as monomers, and 2,4,6-triaminopyrimidine as a cross-linking agent was produced with enhanced mechanical properties.[135,136] Rohacell foams are closed-cell foams with high densities based on polymethacrylimide chemistry. They are generally used as core material because of their excellent heat resistance and mechanical properties to absorb impact force, support structure, and rotorcraft and aircraft parts.[137-140] Overall, the crosslinked aromatic polyester nanocomposites in foam configurations, upon reaching technological maturity, can potentially be implemented where polyimide foams are used today.

,

Acknowledgments

We acknowledge characterization instruments provided at Frederick Seitz Materials Research Laboratory, Beckman Institute for Advanced Science and Technology, Mechanical Testing Instructional Laboratory, and Nuclear Magnetic Resonance/Electron Paramagnetic Resonance (NMR/EPR) Laboratory at the University of Illinois at Urbana-Champaign. We sincerely acknowledge the help of our collaborators listed as co-authors in the articles presented in this work (listed alphabetically); Dr. Adem Kocyigit (Igdir University, Turkey), Dr. Andre Sutrisno (NMR/EPR Laboratory, Illinois), Christine Henderson (Bureau of Reclamation, University of Denver), Dr. Ersin Bahceci (Iskenderun Technical University, Turkey), Dr. Irina Hussainova (Tallinn University of Technology, Estonia), Junho Oh (Department of Mechanical Science and Engineering, Illinois), Dr. Maciej Kumosa (University of Denver), Mohamed Elhebeary (Department of Mechanical Science and Engineering, Illinois), Dr. Munir Nayfeh (Department of Physics, Illinois), Dr. Nenad Miljkovic (Department of Mechanical Science and Engineering, Illinois), and Osman Cifci (Department of Materials Science and Engineering, Illinois). M.B. and I.J. gratefully acknowledge funding from the National Science Foundation (NSF) I/UCRC grant (IIP-1362146). M.B. acknowledges Non-Academic Internship (INTERN) award from the NSF under I/UCRC grant (IIP-1362146) grant.

Disclaimer

Information in this paper may not be used for advertising or promotional purposes. The data and findings should not be construed as an endorsement of any product or firm by Digital Materials LLC and ATSP Innovations.

,

Additional Information

The authors declare no competing interests.

,

References

1. J. Njuguna, K. Pielichowski and J. Fan, *Advances in Polymer Nanocomposites,* **2012**, 472.
2. M. Moniruzzaman and K. I. Winey, *Macromolecules,* **2006**, 39(16), 5194.
3. P. Steurer, R. Wissert, R. Thomann and R. Mülhaupt, *Macromolecular Rapid Communications*, **2009**, 30, 316.
4. S. Sathyanarayana and C. Hübner, Structural Nanocomposites. Engineering Materials. Springer, Berlin, Heidelberg. **2013.**
5. H. Koerner, G. Price, N.A. Pearce, M. Alexander and R.A. Vaia, *Nature Materials*, **2004**, 3(2), 115.
6. P. Song, Z. Cao, Y. Cai, L. Zhao, Z. Fang and S. Fu, *Polymer*, **2011**, 52(18), 4001.
7. E.V. Kuvardina, L.A. Novokshonova, S.M. Lomakin, S.A. Timan and I.A. Tchmutin, *Journal of Applied Polymer Science*, **2013**, 128, 1417.
8. J. Wang, H. Hu, X. Wang, C. Xu, M. Zhang and X. Shang, *Journal of Applied Polymer Science*, **2011**, 122, 1866.
9. H. Hu, X. Wang, J. Wang, L. Wan, F. Liu, H. Zheng, R. Chen and C. Xu, *Chemical Physics Letters*, **2010**, 484, 247.
10. F. Beckert, A.M. Rostas, R. Thomann, S. Weber, E. Schleicher, C. Friedrich and R. Mülhaupt, *Macromolecules*, **2013**, 46, 5488.
11. L. Song, H. Zhang, Z. Zhang and S. Xie, *Composites Part A: Applied Science and Manufacturing*, **2007**, 38(2), 388.
12. Y.F. Zhao, M. Xiao, S.J. Wang, X.C. Ge and Y.Z. Meng, *Composites Science and Technology*, **2007**, 67, 2528.
13. A. Zandiatashbar, R.C. Picu and N. Koratkar, *Journal of Engineering Materials and Technology*, **2012**, 134, 031011.
14. D.R. Bortz, E.G. Heras and I. Martin-Gullon, *Macromolecules*, **2012**, 45, 238.
15. G.Y. Kim, M.-C. Choi, D. Lee and C.-S. Ha, *Macromolecular Materials and Engineering*, **2012**, 297, 303.
16. W. Ma, L. Wu, D. Zhang and S. Wang, *Colloid and Polymer Science*, **2013**, 291, 2765.
17. Y. Li, D. Pan, S. Chen, Q. Wang, G. Pan, and T. Wang. *Materials & Design*, **2013**, 47, 850.
18. D. Frich, K. Goranov, L, Schneggenburger and J. Economy, *Macromolecules*, **1996**, 29 (24), 7734.
19. D. J. Frich, University of Illinois at Urbana-Champaign, **1996**.
20. D. Frich and J. Economy, *Journal of Polymer Science Part A: Polymer Chemistry*, **1997**, 35 (6), 1061.
21. J. Economy and Z. Parkar, *American Chemical Society*, **2011**, 1080, 93.
22. B. Vaezian, J. L. Meyer and J. Economy, *Polymers for Advanced Technologies*, **2016**, 27 (8), 1006.

,

23. W. Wang, J. L. Meyer, Q. Zeng, M. Li, B. Vaezian and J. Economy, *Polymers for Advanced Technologies*, **2016**, 27 (12), 1577.
24. P. Lan, J. L. Meyer, J. Economy and A. A. Polycarpou, *Tribology Letters*, **2015**, 61 (1), 10.
25. P. Lan, J. L. Meyer, B. Vaezian and A. A. Polycarpou, *Wear*, **2016**, 354-355, 10.
26. P. Lan, R. Gheisari, J. L. Meyer and A. A. Polycarpou, *Wear*, **2018**, 398-399, 47.
27. F. F. Shi, L. A. Schneggenburger and J. Economy, *Journal of Applied Polymer Science*, **1997**, 63 (9), 1199.
28. L. A. Schneggenburger, University of Illinois at Urbana-Champaign, **1998**.
29. F. F. Shi and J. Economy, *Journal of Polymer Science Part B: Polymer Physics*, **1998**, 36 (6), 1025.
30. D. Frich, J. Economy and K. Goranov, *Polymer Engineering & Science*, **1997**, 37 (3), 541.
31. D. Frich, A. Hall and J. Economy, *Macromolecular Chemistry and Physics*, **1998**, 199 (5), 913.
32. J. C. Selby, M. A. Shannon, K. Xu and J. Economy, *Journal of Micromechanics and Microengineering*, **2001**, 11 (6), 672.
33. K. Xu, J. C. Selby, M. A. Shannon and J. Economy, *Journal of Applied Polymer Science*, **2004**, 92 (6), 3843.
34. Y. Huang, J. J. McCormick and J. Economy, *Polymers for Advanced Technologies*, **2005**, 16 (1), 1.
35. N. G. Demas, J. Zhang, A. A. Polycarpou and J. Economy, *Tribology Letters*, **2008**, 29 (3), 253.
36. J. Zhang, N. G. Demas, A. A. Polycarpou and J. Economy, *Polymers for Advanced Technologies*, **2008**, 19 (8), 1105.
37. Z. Parkar, University of Illinois at Urbana-Champaign, **2011**.
38. Z. Parkar, C. Mangun, D. King, T. Field, G. Sutton and J. Economy, *Journal of Composite Materials*, **2012**, 46 (15), 1819.
39. J.L. Meyer, M. Bakir, P. Lan, J. Economy, I. Jasiuk, G. Bonhomme and A.A. Polycarpou, *Macromolecular Materials and Engineering*, **2019**, 304(4), 1800647.
40. H. Duran, B. Yameen, M. Geuss, M. Kappl, M. Steinharte and W. Knollf, *Journal of Materials Chemistry C*, **2013**, 1, 7758.
41. M. Bakir, J. L. Meyer, J. Economy and I. Jasiuk, *Macromolecules*, **2016**, 49 (17), 6489.
42. V.P. Shastri, I. Martin and R. Langer, *Proceedings of the National Academy of Sciences of the United States of America*, **2000**, 97 (5), 1970.
43. N.N. Najib, Z.M. Ariff, A.A. Bakar and C.S. Sipaut, *Materials&Design*, **2011**, 32 (2), 505.
44. W. Jackson Jr and H. Kuhfuss, *Journal of Polymer Science Part A: Polymer Chemistry*, **1996**, 34 (15), 3031.
45. K. Xu, University of Illinois at Urbana-Champaign, 1994.
46. J.D. Carter, *Macromolecules*, **1991**, 24(19), 5251.

,

47. M. Bakir, E. Bahceci, J. L. Meyer, J. Economy and I. Jasiuk, *Materials Letters*, **2017**, 196, 288.
48. V. Deshpande and N. Fleck, *International Journal of Impact Engineering*, **2000**, 24(3), 277.
49. L. Di Landro, G. Sala and D. Olivieri, Polymer Testing, **2002**, 21(2), 217.
50. M.A. Hazizan and W. Cantwell, *Composites Part B: Engineering*, 2002, 33(3), 193.
51. M. Bakir, J. L. Meyer, J. Economy and I. Jasiuk, *Polymer*, **2017**, 123, 311.
52. L. Jaouen, A. Renault and M. Deverge, *Applied Acoustics*, **2008**, 69(12), 1129.
53. B. Wicklein, A. Kocjan, G. Salazar-Alvarez, F. Carosio, G. Camino, M. Antonietti and L. Bergström, *Nature Nanotechnology*, **2015**, 10(3), 277.
54. Z. Chen, C. Xu, C. Ma, W. Ren and H.-M. Cheng, *Advanced Materials*, **2013**, 25(9), 1296.
55. V. Eswaraiah, V. Sankaranarayanan and S. Ramaprabhu, *Macromolecular Materials and Engineering*, **2011**, 296(10), 894.
56. R. Andrews, D. Jacques, M. Minot and T. Rantell, *Macromolecular Materials and Engineering*, **2002,** 287(6), 395.
57. A. I. Zhbanov, E. G. Pogorelov and Y.-C. Chang, *ACS Nano*, **2010**, 4 (10), 5937.
58. R. Andrews, D. Jacques, M. Minot and T. Rantell, *Macromolecular Materials and Engineering*, **2002**, 287 (6), 395.
59. A. Yasmin, J.-J. Luo and I. M. Daniel, *Composites Science and Technology*, **2006**, 66 (9), 1182.
60. N. Yousefi, X. Sun, X. Lin, X. Shen, J. Jia, B. Zhang, B. Tang, M. Chan and J. K. Kim, *Advanced Materials*, **2014**, 26 (31), 5480.
61. M. Bakir, J. L. Meyer, A. Sutrisno, J. Economy and I. Jasiuk, *RSC Advances*, **2018**, 8 (9), 4946.
62. S. Kale, F. A. Sabet, I. Jasiuk and M. Ostoja-Starzewski, *Journal of Applied Physics*, **2015**, 118 (15), 154306.
63. A. V. Kyrylyuk and P. van der Schoot, *Proceedings of the National Academy of Sciences*, **2008**, 105 (24), 8221.
64. F. Wang, L. T. Drzal, Y. Qin and Z. Huang, *Journal of Materials Science*, **2015**, 50, 1082.
65. P. Pötschke, T. Fornes and D. Paul, *Polymer*, **2002**, 43 (11), 3247.
66. S. Bhama and S.I. Stupp, *Polymer Engineering and Science*, **1990**, 30, 603.
67. S. Bhama and S.I. Stupp, *Polymer Engineering and Science*, **1990**, 30, 228.
68. S. Biswas, H. Fukushima and L.T. Drzal, *Composites Part A: Applied Science and Manufacturing*, **2011**, 42, 371.
69. S. Lu, S. Li, J. Yu, Z. Yuan and B. Qi, *RSC Advances*, **2013**, 3, 8915.
70. M. Bakir, M. Elhebeary, J. L. Meyer, A. Sutrisno, J. Economy and I. Jasiuk, *Journal of Applied Polymer Science*, **2018**, 135 (32), 46584.
71. A. M. Donald, A. H. Windle and S. Hanna, Cambridge University Press, **2006**.
72. C. Velasco-Santos, A. L. Martínez-Hernández, F. T. Fisher, R. Ruoff and V. M. Castano, *Chemistry of Materials*, **2003**, 15 (23), 4470.

,

73. M. Bakir, J. L. Meyer, A. Sutrisno, J. Economy, and I. Jasiuk, *Journal of Polymer Science Part B: Polymer Physics*, **2018**, 56(24), 1595.
74. H. Oh and P. F. Green, *Nature Materials*, **2009**, 8 (2), 139.
75. H. Kim, A. A. Abdala and C. W. Macosko, *Macromolecules*, **2010**, 43 (16), 6515.
76. T. Ramanathan, A. Abdala, S. Stankovich, D. Dikin, M. Herrera-Alonso, R. Piner, D. Adamson, H. Schniepp, X. Chen, R. Ruoff, S. T. Nguyen, I. A. Aksay, R. K. Prud'Homme and L. C. Brinson, *Nature Nanotechnology*, **2008**, 3 (6), 327.
77. A. Bansal, H. Yang, C. Li, K. Cho, B. C. Benicewicz, S. K. Kumar and L. S. Schadler, *Nature Materials*, **2005**, 4 (9), 693.
78. J. McMurry, Organic Chemistry, 8th Edition, Brooks Cole, 2011.
79. W. Jackson and H. Kuhfuss, *Journal of Polymer Science. Part A Polymer Chemistry*, **1996**, 34, 3031.
80. T. Davies, *Interscience*, **1964**, 553.
81. M. Bakir, C. N. Henderson, J. L. Meyer, J. Oh, N. Miljkovic, M. Kumosa, J. Economy and I. Jasiuk, *Polymer Degradation and Stability*, **2018**, 147, 49.
82. P.M. Hergenrother, *High Performance Polymers*, **2003**, 15 (1), 3.
83. J.C. Seferis, *Polymer Composites*, **1986**, 7(3), 158.
84. R.L. Fusaro, *ASLE Transactions*, **1978**, 21(2), 125.
85. E.S. Weiser, T.F. Johnson, T.L. St Clair, Y. Echigo, H. Kaneshiro and B.W. Grimsley, *High Performance Polymers*, **2000**, 12(1), 1.
86. L.M. Robeson, W.F. Burgoyne, M. Langsam, A.C. Savoca and C.F. Tien, *Polymer*, **1994**, 35(23), 4970.
87. J. Vrentas and J. Duda, *Journal of Polymer Science: Polymer Physics Edition*, **1977**, 15 (3), 403.
88. J. Vrentas and J. Duda, D, *Macromolecules*, **1976**, 9 (5), 785.
89. S. Li, R. Vatanparast and H. Lemmetyinen, *Polymer*, **2000**, 41 (15), 5571.
90. G. Hong, Y. Han, T. M. Schutzius, Y. Wang, Y. Pan, M. Hu, J. Jie, C. S. Sharma, U. Müller and D. Poulikakos, *Nano Letters*, **2016**, 16 (7), 4447.
91. M. Munz, C. E. Giusca, R. L. Myers-Ward, D. K. Gaskill and O. Kazakova, *ACS Nano*, **2015**, 9 (8), 8401.
92. S. Wang, Y. Zhang, N. Abidi and L. Cabrales, *Langmuir*, **2009**, 25 (18), 11078.
93. C. Bao, L. Song, W. Xing, B. Yuan, C. A. Wilkie, J. Huang, Y. Guo and Y. Hu, *Journal of Materials Chemistry*, **2012**, 22 (13), 6088.
94. L. Li, C. Y. Li and C. Ni, *Journal of the American Chemical Society*, **2006**, 128, 1692.
95. Y. Takenaka, H. Miyaji, A. Hoshino, A. Tracz, J. K. Jeszka and I. Kucinska, *Macromolecules*, **2004**, 37, 9667.
96. M. M. L. Arras, R. Jana, M. Mühlstädt, S. Maenz, J. Andrews, Z. Su, C. Grasl and K. D. Jandt, *Macromolecules*, **2016**, 49, 3550.
97. S. Zhang, W. Lin, C.-P. Wong, D. G. Bucknall and S. Kumar, *ACS Applied Materials and Interfaces*, **2010**, 2, 1642.

,

98. H. Yue, A. Monreal-Bernal, J. P. Fernández-Blázquez, J. Llorca and J. J. Vilatela, *Scientific Reports*, **2015**, 5, 16729.
99. M. Bakir, J. L. Meyer, I. Hussainova, A. Sutrisno, J. Economy and I. Jasiuk, *Macromolecular Chemistry and Physics*, **2017**, 218 (24), 1700338.
100. L. Li, C. Y. Li and C Ni, *Journal of the American Chemical Society*, **2006**, 128 (5), 1692.
101. E. D. Laird and C. Y. Li, *Macromolecules*, **2013**, 46 (8), 2877.
102. L. Li, C. Y. Li, C. Ni, L. Rong and B. Hsiao, *Polymer*, **2007**, 48 (12), 3452.
103. S. Haefner, M. Benzaquen, O. Bäumchen, T. Salez, R. Peters, J. D. McGraw, K. Jacobs, E. Raphaël and K. Dalnoki-Veress, *Nature Communications*, **2015**, 6, 7409.
104. C. B. Kim, J. C. Wistrom, H. Ha, S. X. Zhou, R. Katsumata, A. R. Jones, D. W. Janes, K. M. Miller and C. J. Ellison, *Macromolecules*, **2016**, 49, 7069.
105. A. L. Yarin, W. Liu and D. H. Reneker, *Journal of Applied Physics*, **2002**, 91, 4751.
106. A. Espinoza-Martínez, C. Avila-Orta, V. Cruz-Delgado, O. Olvera-Neria, J. González-Torres and F. Medellín-Rodríguez, *Journal of Nanomaterials*, **2012**, 2012, 189820.
107. J.A. Fernandes, Y. Morisaki and Y. Chujo, *Polymer Journal*, **2011**, 43, 733.
108. C.-H.M. Chuang, P.R. Brown, V. Bulović and M.G. Bawendi, Nature Materials, **2014**, 13, 796.
109. J. Bao and M.G. Bawendi, *Nature*, **2015**, 523, 67.
110. N.D. Bronstein, Y. Yao, L. Xu, E. O'Brien, A.S. Powers, V.E. Ferry, A.P. Alivisatos and R.G. Nuzzo, *ACS Photonics*, **2015**, 2, 1576.
111. O.E. Semonin, J.M. Luther and M.C. Beard, *Materials Today*, **2012**, 15, 508.
112. A. Kocyigit, M. Bakir, O. S. Cifci, B. Enders, I. Jasiuk and M. H. Nayfeh, *European Polymer Journal*, **2018**, 103, 351.
113. S.-H. Kim, Y.-H. Kim, H.-N. Cho, S.-K. Kwon, H.-K. Kim and S.-K. Choi, *Macromolecules*, **1996**, 29 (16), 5422.
114. E. V. Rogozhina, D. A. Eckhoff, E. Gratton and P. V. Braun, *Journal of Materials Chemistry*, **2006**, 16 (15), 1421.
115. C. S. Cucinotta, A. Ruini, M. J. Caldas and E. Molinari, *The Journal of Physical Chemistry B*, **2004**, 108 (45), 17278.
116. M. Darder, P. Aranda and E. Ruiz-Hitzky, *Advanced Materials*, **2007**, 19, 1309.
117. B. Gasser, *Injury*, **2000,** 31, 48.
118. K. Rezwan, Q.Z. Chen, J.J. Blaker and A.R. Boccaccini, *Biomaterials*, **2006**, 27, 3413.
119. M. Bakir, J. L. Meyer, A. Sutrisno, J. Economy and I. Jasiuk, *Scientific Reports*, **2018**, 8 (1), 14869.
120. Y. Huang and J. Economy, *MRS Proceedings*, **2011**, 1063.
121. N. D. Luong, U. Hippi, J. T. Korhonen, A. J. Soininen, J. Ruokolainen, L.-S. Johansson, J.-D. Nam and J. Seppälä, *Polymer*, **2011**, 52 (23), 5237.
122. X. Zhao, Q. Zhang, D. Chen and P. Lu, *Macromolecules*, **2010**, 43 (5), 2357.
123. L. Chen, K. Zheng, X. Tian, K. Hu, R. Wang, C. Liu, Y. Li and P. Cui, *Macromolecules*, **2009**, 43 (2), 1076.

,

124. A. Bain, D. Eaton, A. Hamielec, M. Mlekuz, and B. Sayer, *Macromolecules*, **1989**, 22 (9), 3561.
125. M.T. Masood, E.L. Papadopoulou, J.A. Heredia-Guerrero, I.S. Bayer, A. Athanassiou, and L. Ceseracciu, *Carbon*, **2017**, 123, 26.
126. D. Liu, W. Zhao, S. Liu, Q. Cen and Q. Xue, *Surface and Coatings Technology*, **2016**, 286, 354.
127. K. Bashandeh, P. Lan, J.L. Meyer, A.A. Polycarpou, *Tribology Letters*, **2019**, 67, 99.
128. T.-M.J. Richardson, D. Jan, J. Hogan, G. Palmer, B. Koss, J. Samson, R. Huang and J. Know, 45th International Conference on Environmental Systems, **2015**.
129. J.T. O'neill, U.S. Patent 4,488,619, **1984**.
130. S.K. Drost, U.S. Patent 7,410,126, **2008**.
131. F.Y. Hshieh, D.B. Hirsch and H.D. Beeson, *Fire and Materials*, **2003**, 27(3), 119.
132. G. Bitetti, S. Mileti and M. Marchetti, *Journal of Spacecraft and Rockets*, **2009**, 46(1), 210.
133. E.S. Weiser, T.F. Johnson, T.L. St Clair, Y. Echigo, H. Kaneshiro and B.W.Grimsley, *High Performance Polymers*, **2000**, 12(1), 1.
134. M.K. Williams, E.S. Weiser, J.E. Fesmire, B.W. Grimsley, T.M. Smith, J.R. Brenner and G.L. Nelson, *Polymers for Advanced Technologies*, **2005**, 16(2-3), 167.
135. H.J. Chu, B.K. Zhu, Y.Y. Xu, *Journal of Applied Polymer Science*, **2006**, 102(2), 1734.
136. H.J. Chu, B.K. Zhu, Y.Y. Xu, *Polymers for Advanced Technologies*, **2006**, 17(5), 366.
137. Q.M. Li, R.A.W. Mines and R.S. Birch, *International Journal of Solids and Structures*, **2000**, 37(43), 6321.
138. D. Benderly and S. Putter, *Polymer Testing*, **2004**, 23(1), 51.
139. E. Bosze, J. Simon-Gillo, J. Boissevain, J. Chang and R. Seto, *Nuclear Instruments and Methods in Physics Research Section A: Accelerators, Spectrometers, Detectors and Associated Equipment*, **1997**, 400(2-3), 224.
140. H.F. Seibert, *Reinforced Plastics*, **2006**, 50(1), 44.